Construction of spinel/perovskite heterojunction for boosting photocatalytic performance for polyacrylamide

Qinghan Zhu[1], Yuxue Luo[1], Ke Yang[1], Guangbo Che[2], Haiwang Wang[1,*], Jian Qi[3,4*]

1 Key Laboratory of Dielectric and Electrolyte Functional Material Hebei Province, Northeastern University at Qinhuangdao, Qinhuangdao, China 066004; zhuqinghan0110@163.com (Q.Z.); luoyuxue2001@163.com (Y.L.); y1210620501@163.com (K.Y.)

2 College of Chemistry, Baicheng Normal University, Baicheng, China 137000; guangboche@bcnu.edu.cn

3 State Key Laboratory of Biochemical Engineering, Institute of Process Engineering, Chinese Academy of Sciences, Beijing, China 100190

4 School of Chemical Engineering, University of Chinese Academy of Sciences, Beijing, China 100049

* Correspondence: whwdbdx@neuq.edu.cn (H.W.); jqi@ipe.ac.cn (J.Q.)

Adsorption capacity test of $ZnFe_2O_4/Ba_{0.7}Sr_{0.3}TiO_3$ (ZFO wt%=31) on PAM:

A 50 mg ZFO-BST sample was taken and added to a 60 ml of 100 mg/L PAM solution. The suspension was stirred in the dark for 30 minutes and the solid and liquid were separated by centrifugation. To minimize errors, the wet sample and test tube were dried at 60 °C for 12 hours together and weighed. The weight of the adsorbed PAM was the difference between the weight before and after drying (the test tube and dry sample were weighed beforehand)

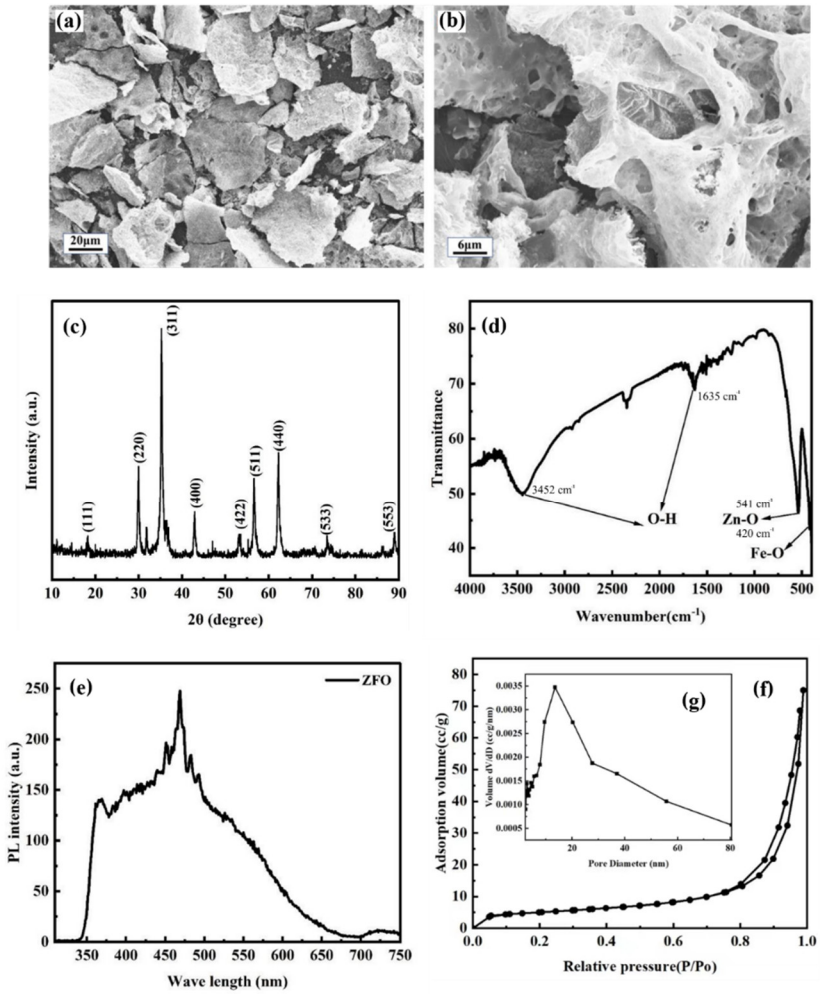

Figure S1. (a, b) SEM images of $ZnFe_2O_4$ samples, (c) XRD diffraction pattern, (d) FT-IR spectrum, (e) PL spectrum, (f) Nitrogen adsorption desorption isotherm, (g) Pore size distribution.

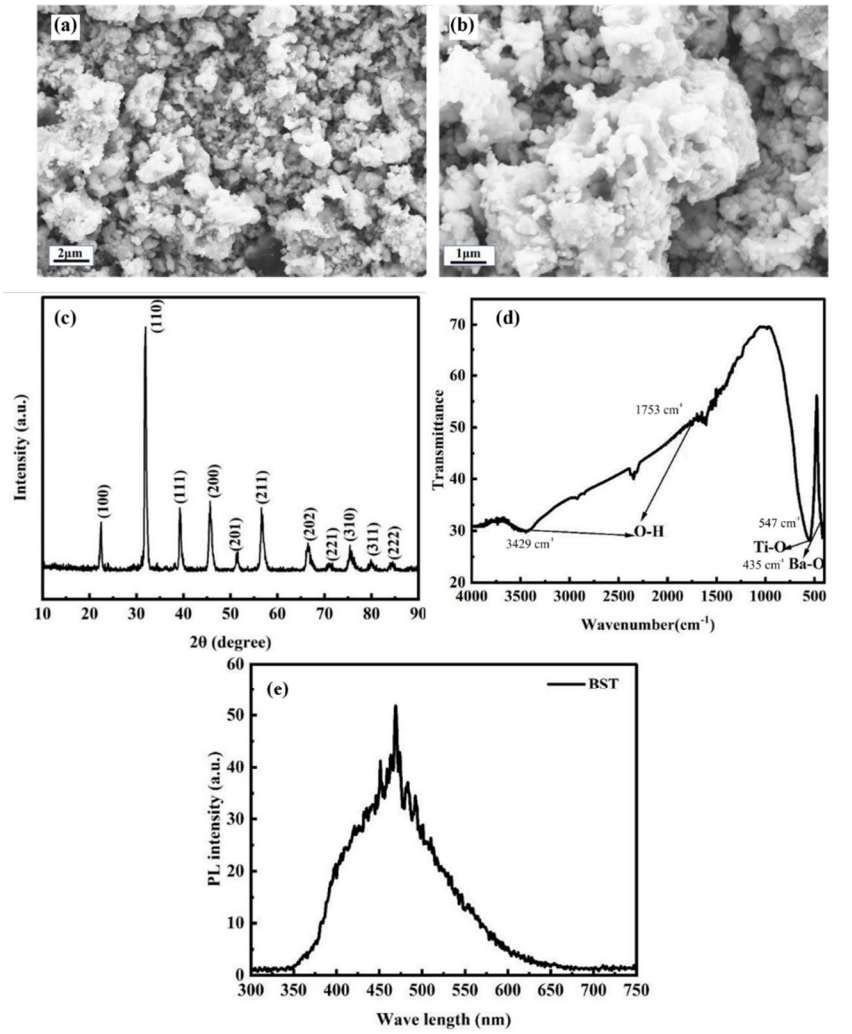

Figure S2. (a, b) SEM images of $Ba_{0.7}Sr_{0.3}TiO_3$, (c) XRD diffraction pattern, (d) FT-IR spectrum, (e) PL spectrum.

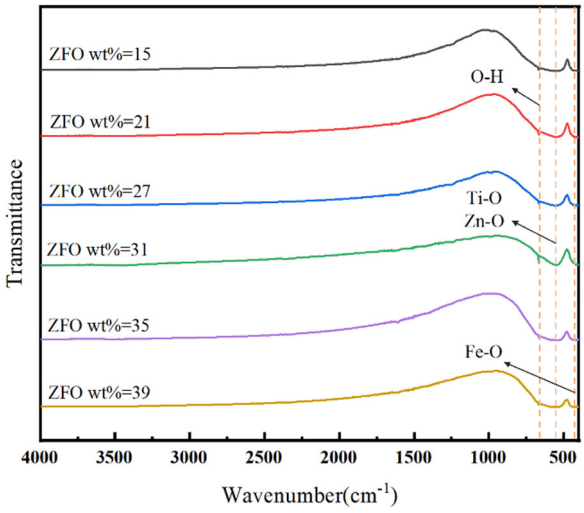

Figure S3. FT-IR spectra of $ZnFe_2O_4/Ba_{0.7}Sr_{0.3}TiO_3$ samples with different components

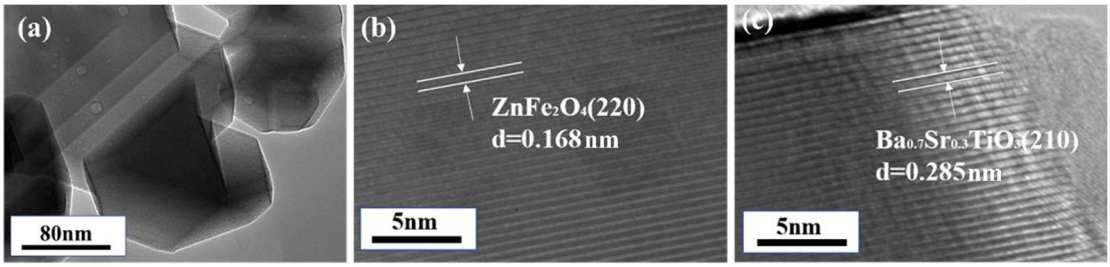

Figure S4. (a) TEM image and (b-c) HRTEM of $ZnFe_2O_4/Ba_{0.7}Sr_{0.3}TiO_3$ (ZFO wt%=31)

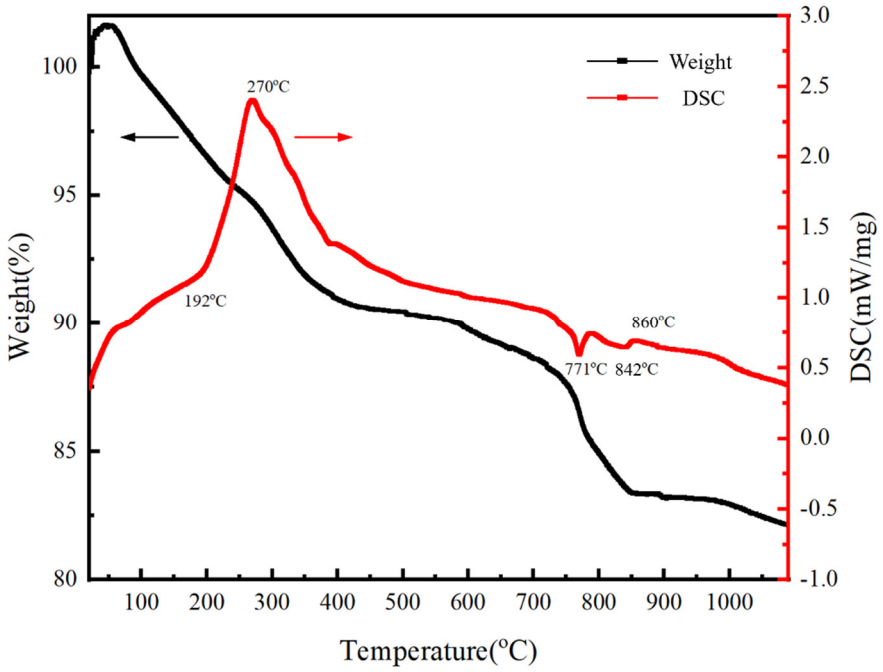

Figure S5. TG-DSC curve of $ZnFe_2O_4/Ba_{0.7}Sr_{0.3}TiO_3$ gel precursor (ZFO wt%=31)

Table S1. Comparison between XRF analysis results and theoretical values of $ZnFe_2O_4/Ba_{0.7}Sr_{0.3}TiO_3$

ZFO wt%	Element	Energy (keV)	Measured value(w/%)	Theoretical value(w/%)
	BaO	4.464	37.17	36.01
	TiO_2	4.511	25.54	26.90
27	Fe_2O_3	6.404	19.37	17.68
	ZnO	8.639	9.752	8.940
	SrO	14.17	8.169	10.49
	BaO	4.464	35.62	33.76
	TiO_2	4.511	23.05	25.22
31	Fe_2O_3	6.404	21.88	20.71
	ZnO	8.639	12.00	10.48
	SrO	14.17	7.450	9.830
	BaO	4.464	33.70	31.78
	TiO_2	4.511	24.06	23.74
35	Fe_2O_3	6.404	22.52	23.39
	ZnO	8.639	12.91	11.84
	SrO	14.17	6.810	9.260

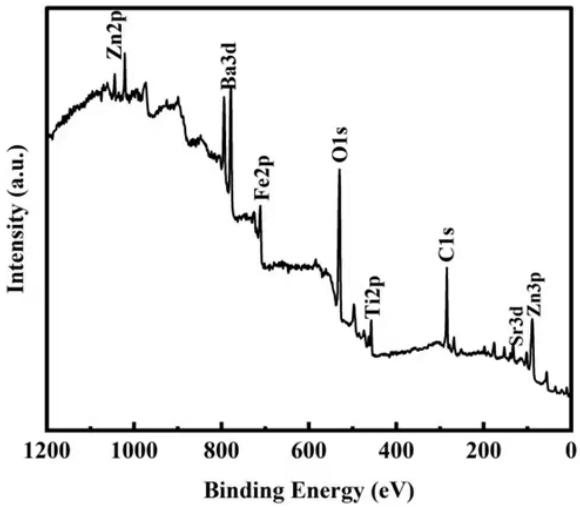

Figure S6. Full XPS spectrum of $ZnFe_2O_4/Ba_{0.7}Sr_{0.3}TiO_3$ sample (ZFO wt%=31)

Table S2. Specific surface area, pore size, and pore volume of $ZnFe_2O_4/Ba_{0.7}Sr_{0.3}TiO_3$ (ZFO wt%=31)

Sample	$S_{BET}/(m^2 \cdot g^{-1})$	Average pore diameter/nm	Pore volume/$(cm^3 \cdot g^{-1})$
$ZnFe_2O_4/Ba_{0.7}Sr_{0.3}TiO_3$	1.85	14.55	0.01

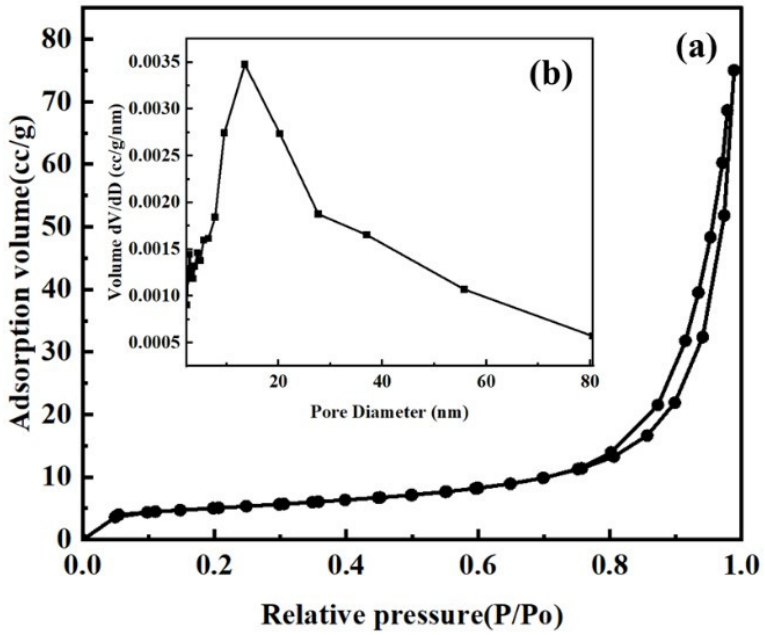

Figure S7. (a) Nitrogen adsorption desorption isotherm and (b) Pore size distribution of $ZnFe_2O_4/Ba_{0.7}Sr_{0.3}TiO_3$ (ZFO wt%=31)

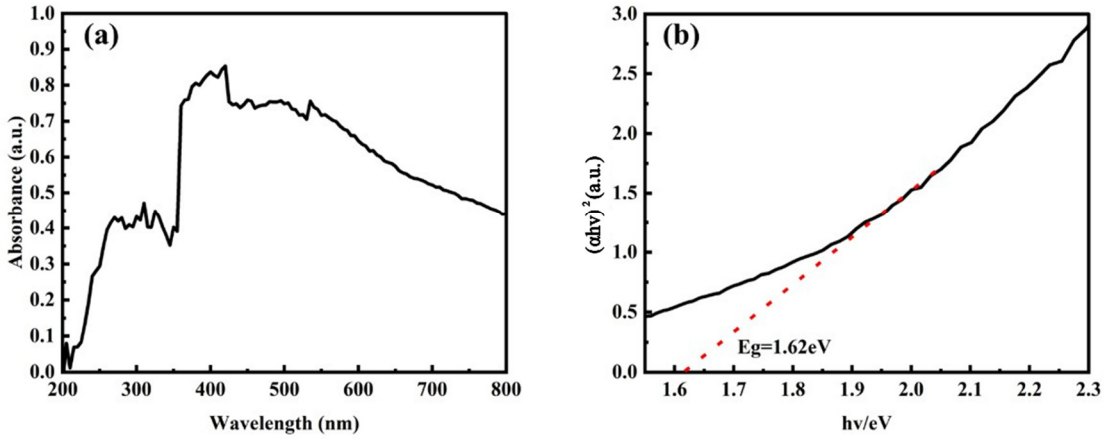

Figure S8. (a) UV-visible absorption spectrum of $ZnFe_2O_4/Ba_{0.7}Sr_{0.3}TiO_3$ (ZFO wt%=31), (b) corresponding Tauc plot curve of (a)

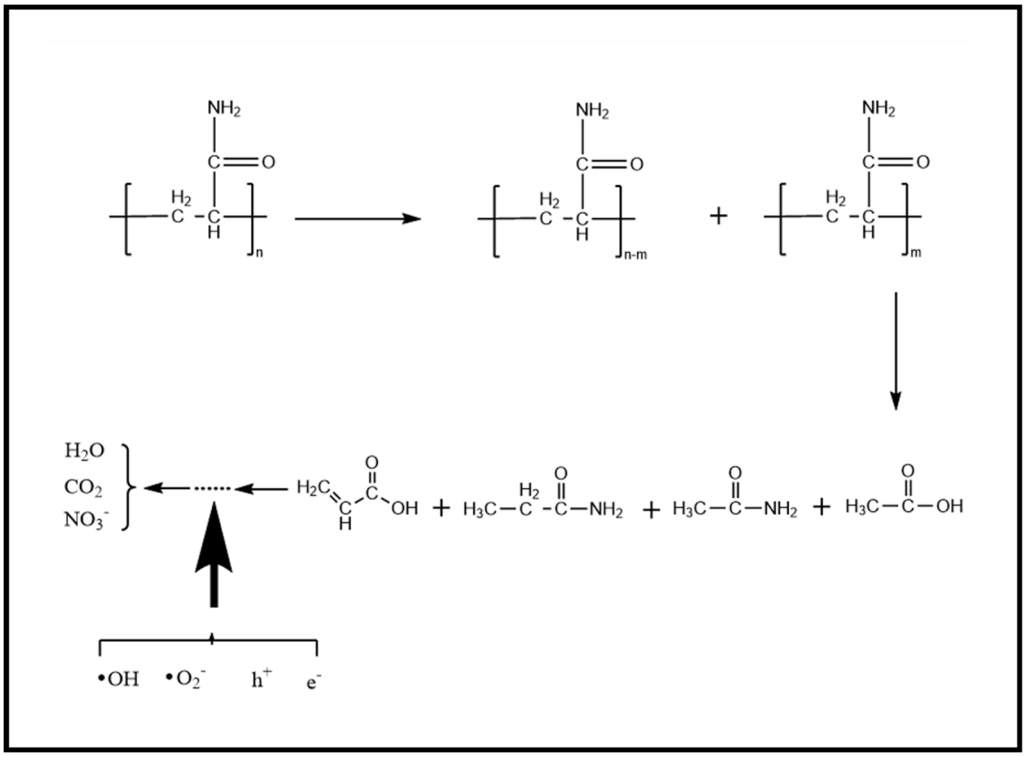

Figure S9. Speculative pathways for photocatalytic degradation of PAM

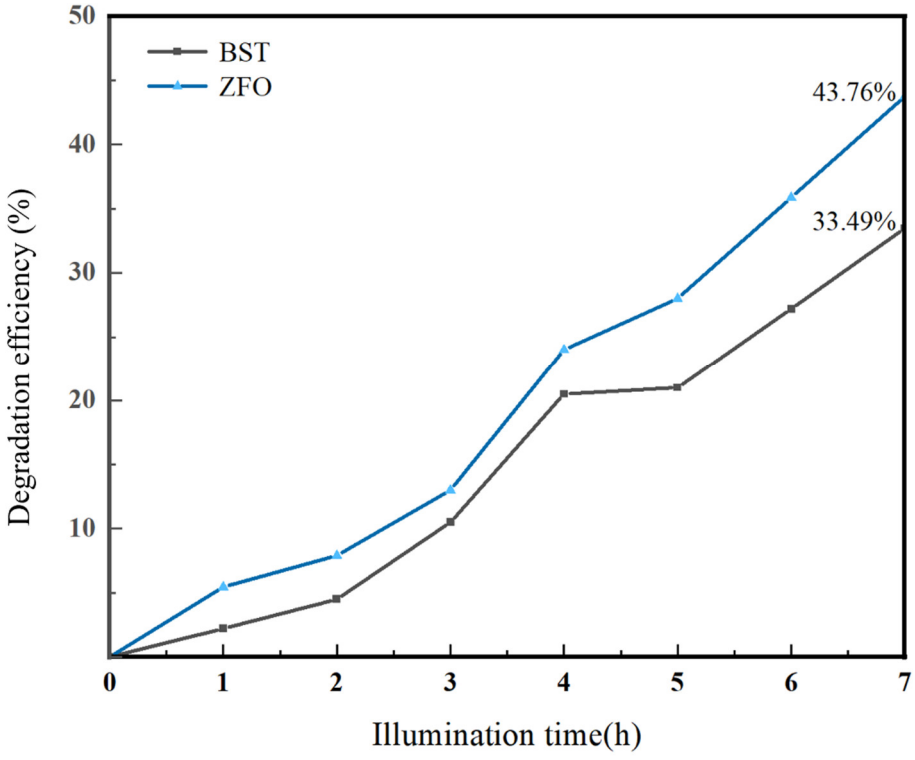

Figure S10. Photodegradation of PAM aqueous solution by $ZnFe_2O_4$ (ZFO) and $Ba_{0.7}Sr_{0.3}TiO_3$ (BST)

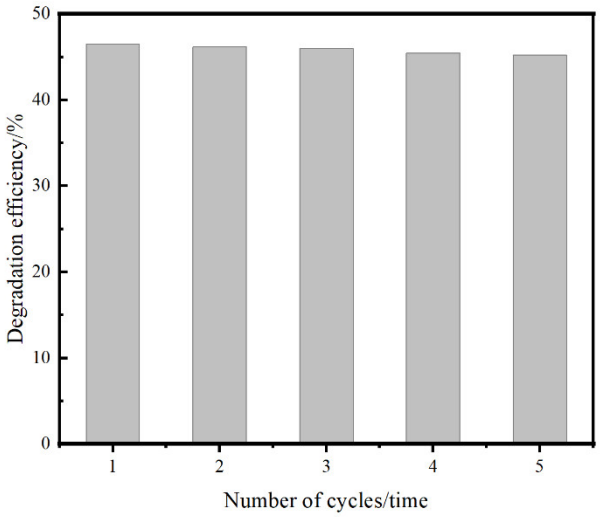

Figure S11. The recycling performance of $ZnFe_2O_4/Ba_{0.7}Sr_{0.3}TiO_3$ (ZFO wt%=31)

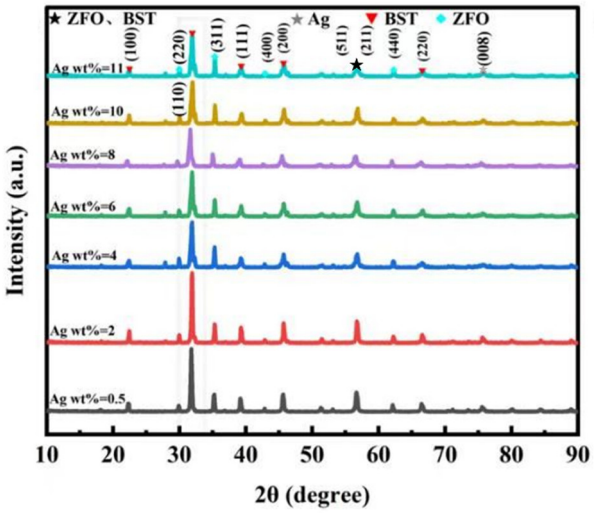

Figure S12. XRD patterns of $ZnFe_2O_4/Ba_{0.7}Sr_{0.3}TiO_3$/Ag with different Ag contents

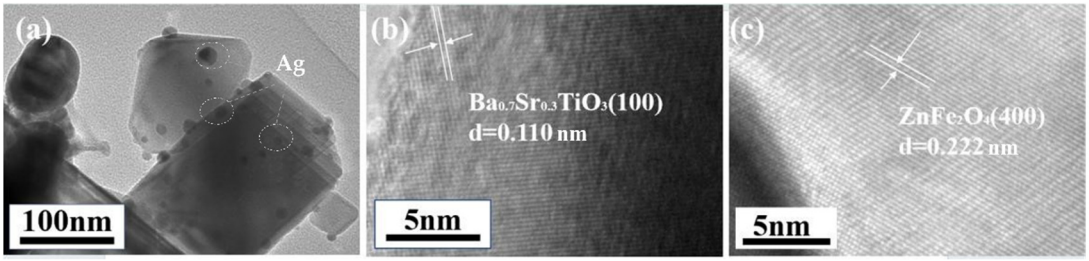

Figure S13. (a) TEM image and (b-c) HRTEM of $ZnFe_2O_4/Ba_{0.7}Sr_{0.3}TiO_3$/Ag (Ag wt%=4)

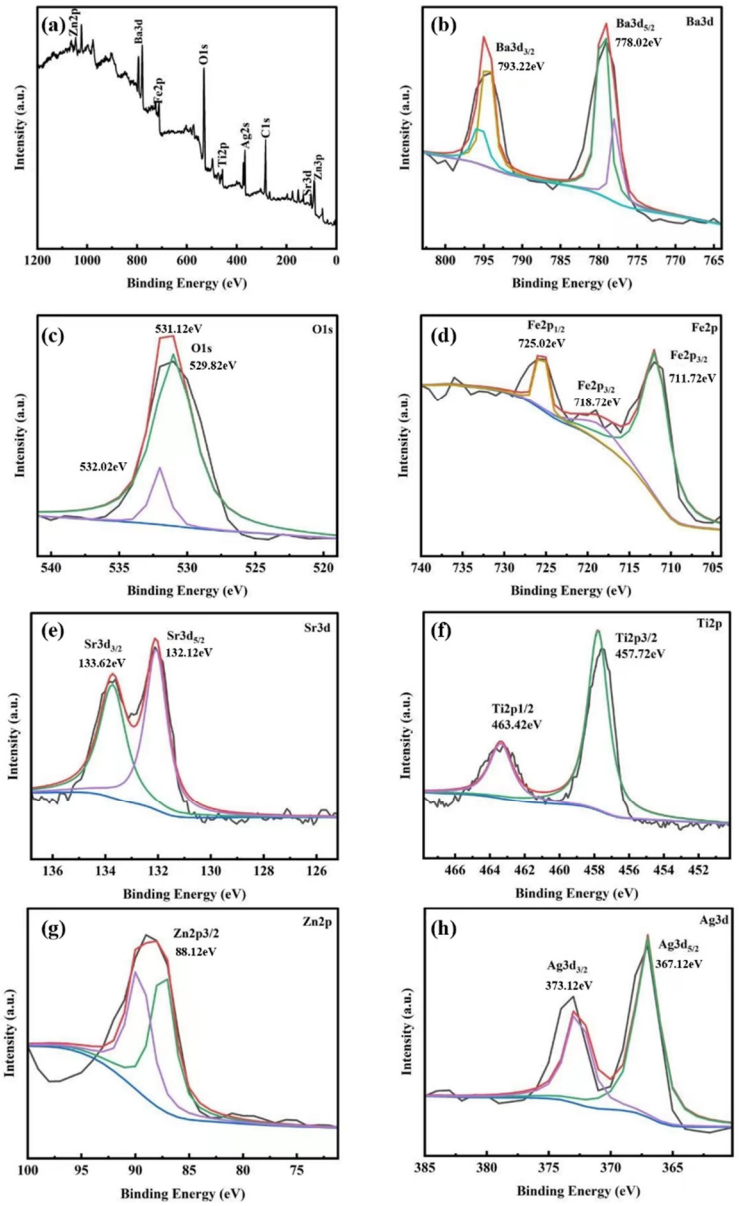

Figure S14. XPS spectra of $ZnFe_2O_4/Ba_{0.7}Sr_{0.3}TiO_3/Ag$: (a) full spectrum, (b) Ba 3d, (c) O 1s, (d) Fe 2p, (e) Sr 3d, (f) Ti 2p, (g) Zn 2p and (h)Ag 3d

Table S3. Specific surface area, pore size, and pore volume of $ZnFe_2O_4/Ba_{0.7}Sr_{0.3}TiO_3/Ag$ (Ag wt%=4)

Sample	$S_{BET}/(m^2 \cdot g^{-1})$	Average pore diameter/nm	Pore volume/$(cm^3 \cdot g^{-1})$
$ZnFe_2O_4/Ba_{0.7}Sr_{0.3}TiO_3/Ag$	2.59	14.65	0.02

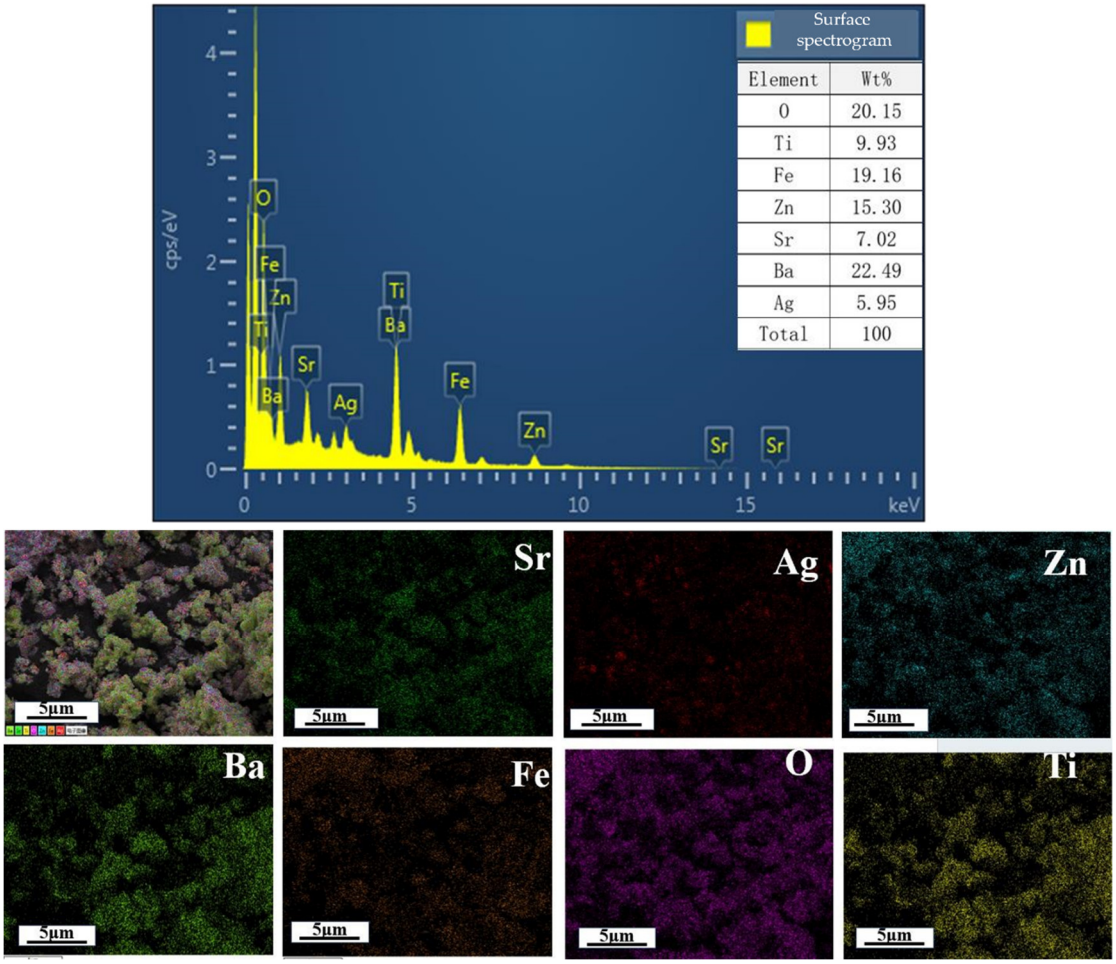

Figure S15. EDS spectra of $ZnFe_2O_4/Ba_{0.7}Sr_{0.3}TiO_3$/Ag (Ag wt%=4)

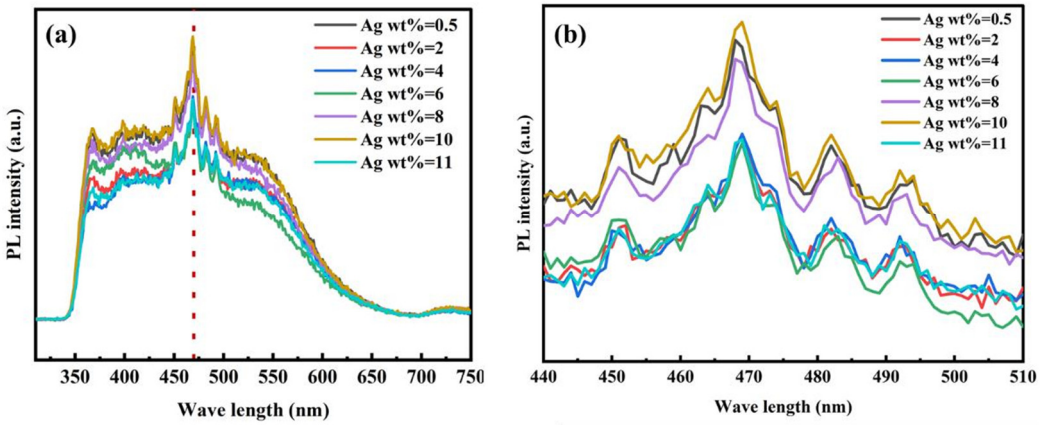

Figure S16. (a) PL spectra of $ZnFe_2O_4/Ba_{0.7}Sr_{0.3}TiO_3$/Ag with different Ag content and (b) Partial enlarged view of (a)

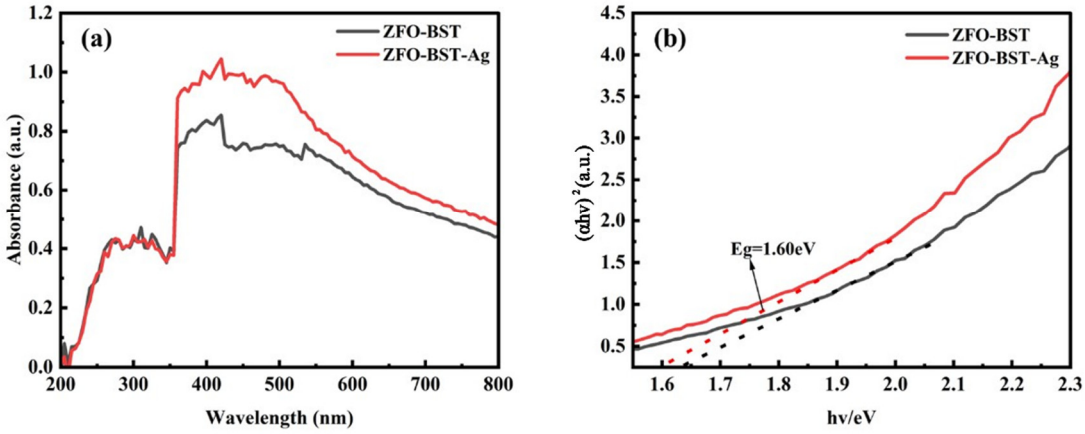

Figure S17. (a) UV-visible absorption spectra of $ZnFe_2O_4/Ba_{0.7}Sr_{0.3}TiO_3$ (ZFO-BST) and $ZnFe_2O_4/Ba_{0.7}Sr_{0.3}TiO_3$/Ag (ZFO-BST-Ag, Ag wt%=4), (b) Corresponding Tauc plot curves of (a)

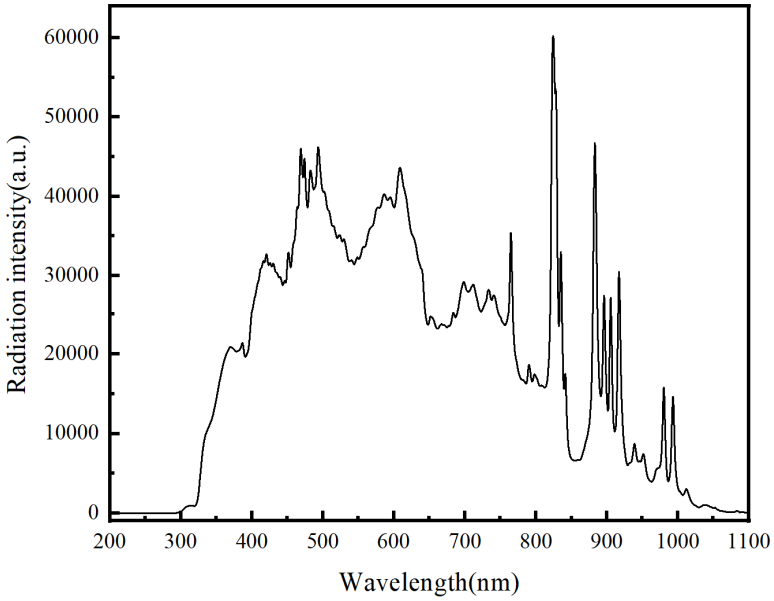

Figure S18. The irradiation spectrum of the xenon lamp

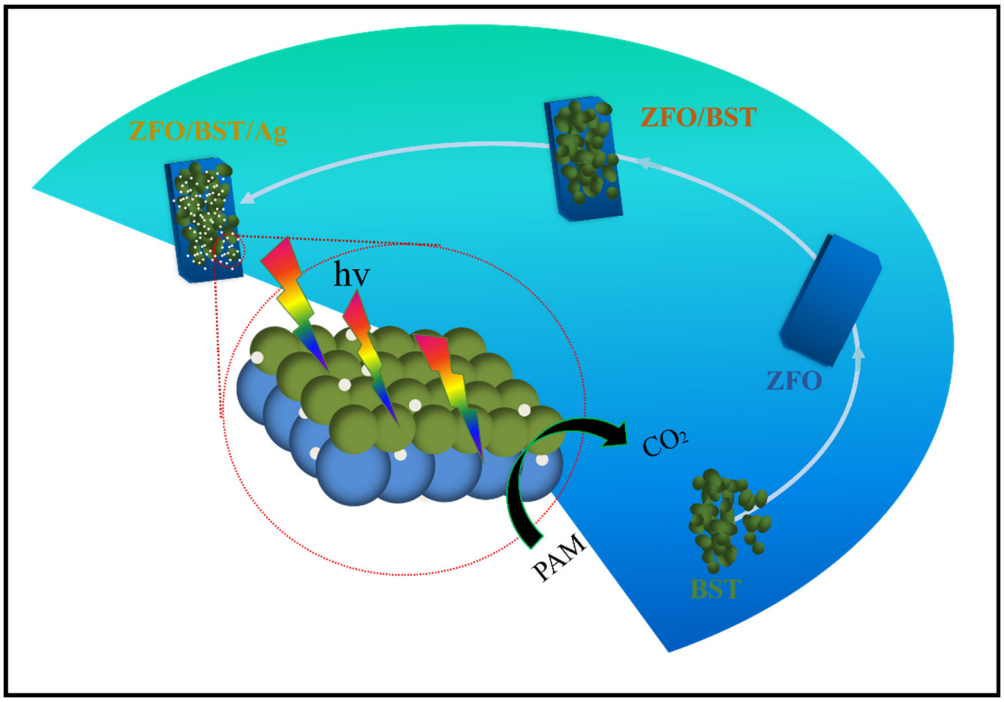

Figure S19. The photocatalytic degradation scheme of $ZnFe_2O_4/Ba_{0.7}Sr_{0.3}TiO_3/Ag$

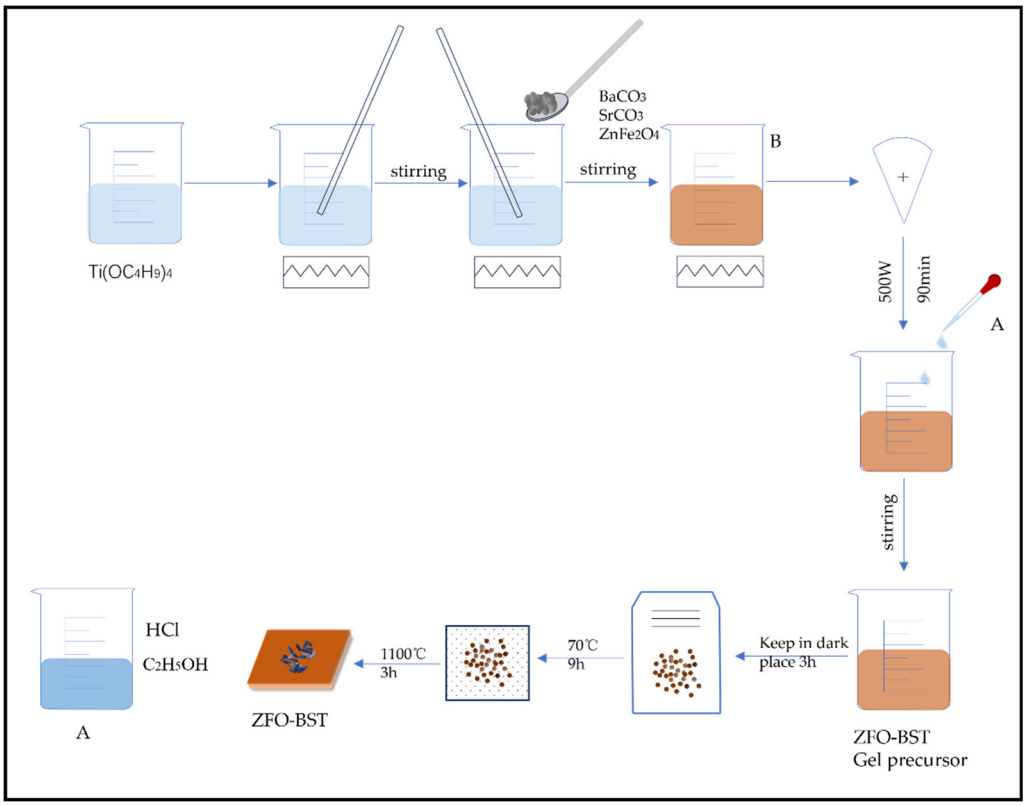

Figure S20. Preparation process diagram of $ZnFe_2O_4/Ba_{0.7}Sr_{0.3}TiO_3$